



Melatonin improves pregnancy outcomes in adenomyosis mice by restoring endometrial receptivity via NF- κ B/apoptosis signaling

Xiaohong Guan¹, Dan Liu², Hong Zhou², Chaoqun Dai³, Tao Wang¹, Yuan Fang¹, Yanping Jia², Kunming Li²

¹Department of Gynecology, Shanghai First Maternity and Infant Hospital, School of Medicine, Tongji University, Shanghai, China; ²Center for Assisted Reproduction Medicine, Shanghai First Maternity and Infant Hospital, School of Medicine, Tongji University, Shanghai, China; ³Department of Pathology, Shanghai First Maternity and Infant Hospital, School of Medicine, Tongji University, Shanghai, China

Contributions: (I) Conception and design: Y Jia, K Li; (II) Administrative support: Y Jia, K Li; (III) Provision of study materials or patients: X Guan; (IV) Collection and assembly of data: X Guan; (V) Data analysis and interpretation: D Liu, H Zhou, C Dai, T Wang, Y Fang; (VI) Manuscript writing: All authors; (VII) Final approval of manuscript: All authors.

Correspondence to: Dr. Kunming Li; Dr. Yanping Jia. Center for Assisted Reproduction Medicine, Shanghai First Maternity and Infant Hospital, School of Medicine, Tongji University, 2699 Gaoke West Road, Pudong District, Shanghai 201204, China. Email: likunming@51mch.com; jianping@tongji.edu.cn.

Background: Adenomyosis is a common gynecological disease which seriously impacts female fertility and is increasing in incidence in women of childbearing age. Melatonin has beneficial effects on reproductive processes. However, its impact on the uterine receptivity of patients with adenomyosis remains unclear. In this study, we investigated the effect of melatonin on uterine receptivity and pregnancy outcomes in an adenomyosis mouse model.

Methods: We induced an adenomyosis mouse model by oral administration of tamoxifen to neonatal female CD-1 mice, then conducted a melatonin injection experiment to investigate its effect on implantation rates (n=6 each). In a second experiment, the endometrium in the implantation state was collected to identify the local action of melatonin on adenomyosis mice (n=6 each), and in a parallel study, the pregnancy rate and number of offspring were recorded (n=6 each).

Results: The number of implantation sites in the adenomyosis model mice was much less than in control group (5.0±2.10 vs. 13.3±2.38, P<0.0001), and 30 mg/kg of melatonin significantly improved this (9.0±0.63 vs. 5.0±2.10, P=0.002). Additionally, melatonin administration ameliorated the impaired endometrial receptivity [leukemia inhibitory factor (LIF), integrin β 3, homeobox A10 (HoxA10), and HoxA11], and improved the endometrium development [endometrial area (EA) and endometrial thickness index (ETI)] and pregnancy outcomes. Furthermore, the expression of implantation-related genes (*Era*, *Pra*, and *P53*), inflammatory factors [tumor necrosis factor- α (TNF- α) and interleukin-1 β (IL-1 β)], oxidative stress associated genes (*Gpx1* and *Sod1*), and apoptosis-related genes or proteins (Bax, Bcl-2, caspase-3, and cleaved caspase-3) was detected. The results showed higher local levels of reactive oxygen species (ROS) and inflammatory cytokines in the uterus of an adenomyosis model mice induced endometrial cells apoptosis and tissue damage, changed the uterine microenvironment, affected embryo implantation, and reduced the fertility of adenomyosis. Interestingly, melatonin significantly mitigated adenomyosis-induced changes by inhibiting the nuclear factor kappa B (NF- κ B) signaling pathway, increasing the vascular endothelial growth factor (VEGF) expression, decreasing the endometrial cells apoptosis, and improving pregnancy outcomes.

Conclusions: Melatonin treatment restored impaired uterine development and endometrial receptivity of adenomyosis mice by improving the endometrial microenvironment via the NF- κ B/apoptosis signaling pathway. Our results provided new insight into melatonin-based therapy for adenomyosis-related infertility.

Keywords: Adenomyosis; infertility; endometrial receptivity; melatonin; nuclear factor kappa B signaling (NF- κ B signaling)

Submitted Oct 18, 2022. Accepted for publication Nov 29, 2022.

doi: 10.21037/atm-22-5493

View this article at: <https://dx.doi.org/10.21037/atm-22-5493>

Introduction

Adenomyosis is characterized by the presence of endometrial glands and stroma within the myometrium and is extremely common in women of reproductive age. The condition has an estimated prevalence of 38–64% (1), and although benign, is both progressive and recurrent (2). Adenomyosis is associated with lifelong infertility, identified in 27–79% of infertile women (3), and compared with controls, involves a 43% reduction in the odds ratio (OR) for clinical pregnancy (4). Recent studies have emphasized adenomyosis as associated with a 30% decrease in the likelihood of pregnancy, with clinical pregnancy rate significantly reduced *in vitro* fertilization/intracytoplasmic sperm injection as compared with control subjects (40.5% vs. 49.8%) (5,6). Although the exact mechanisms by which adenomyosis may limit fertility remain elusive, alterations in endometrial receptivity have been suggested as important causes (7,8).

Clinically and pathologically, adenomyosis is a hormone-dependent condition, which shows eutopic endometrial tissue synthesizes estrogen locally and exhibits progesterone resistance and abnormal cytokine production (7,9). Abnormal endometrial molecular expressions in adenomyosis have been proposed as impairing implantation

and early embryo development. Nuclear factor kappa B (NF- κ B), an inflammatory mediator, was greatly involved in the pathogenesis and progression in adenomyosis (10). When activated, its nuclear translocation triggers many pro-inflammatory cytokines transcription, including interleukin-1 β (IL-1 β), tumor necrosis factor- α (TNF- α), and so on (11). Inflammation processes such as IL-1 β , TNF- α (12,13), natural killer cells, macrophages (14), a spectrum of cytokines (15), and the presence of abnormal levels of intrauterine free radicals have been proposed as inducing cellular and biochemical alterations within the eutopic endometrium. Homeobox A10/11 (HoxA10/11) and leukemia inhibitory factor (LIF) were downregulated in both mice models (16) and the secretory phase endometrium of women with adenomyosis (17), and their dysregulation decreased downstream factors influencing endometrial receptivity by repressing the target gene integrin β 3 (18). Excessive reactive oxygen species (ROS) production activated the expression of Bax, leading to a decrease in mitochondrial membrane potential, which activated caspase cascade and caused apoptosis.

Melatonin (N-acetyl-5-methoxytryptamine) is a powerful antioxidant that has multiple important physiological and pathological functions, including regulation of inflammation, apoptosis, and metabolism (19). It is capable of suppressing the production of pro-inflammatory cytokines, including TNF- α and IL-1 β , mainly by blocking NF- κ B signaling (20). Evidence suggests melatonin can optimize maternal, placental, and fetal physiology (21). It is involved in the maintenance of uterine homeostasis through regulation of numerous pathways associated with uterine receptivity and gestation, and improves uterine physiological processes, such as decidualization and implantation (22). A previous animal study also showed exogenous melatonin treatment can improve mouse embryo implantation and litter size (23). These findings suggest melatonin may be useful for the treatment of subfertility caused by adenomyosis.

However, while it is known to have beneficial effects on reproductive processes, the effect of melatonin on adenomyosis-induced endometrial disorders is poorly understood. In the present study, we adopted an adenomyosis mouse model to investigate whether melatonin

Highlight box

Key findings

- Melatonin could improve the endometrial receptivity in adenomyosis model mice.

What is known and what is new?

- Melatonin has beneficial effects on reproductive processes.
- Whether melatonin has potential impact on endometrial receptivity in adenomyosis remain unclear. In this study, we found melatonin played protective effect on the impaired uterine receptivity in adenomyosis mice.

What is the implication, and what should change now?

- The results demonstrate the protective effect of melatonin on adenomyosis, especially the positive melatonin-specific effects on uterine development and endometrial receptivity. These findings highlight the potential of melatonin as an adjunctive therapy candidate for the treatment of infertility in patients of adenomyosis.

could exert a protective effect on adenomyosis mice and explored the underlying mechanisms. We present the following article in accordance with the ARRIVE reporting checklist (available at <https://atm.amegroups.com/article/view/10.21037/atm-22-5493/rc>).

Methods

Animal model

Animal experiments in this study were approved by the Animal Ethics Committee of Tongji University (No. TJBG01321101) and conducted under the guidelines of the National Research Council's Guide for the Care and Use of Laboratory Animals (24). A protocol was prepared before the study without registration. Female neonatal CD-1 mice (1.8–2.0 g; 13 pregnant mice were provided by Beijing Vital River Laboratory Animal Technology Co., Ltd., Beijing, China) were orally dosed on days 2 through 5 after birth (birth day was set as day 1) with 2.7 $\mu\text{mol/kg}$ tamoxifen (Shanghai Fudan Forward Science & Technology Co., Ltd., Shanghai, China) suspended in a peanut oil/lecithin/condensed milk mixture (2:0.2:3, v/v) at a dose volume of 5 $\mu\text{L/g}$ body weight (16). All mice were housed under controlled conditions of temperature (22–26 °C) and light (12-h/12-h light/dark cycle) with ad libitum access to food and water. After 75 days, tamoxifen-treated mice were randomly assigned into five groups: Group I, adenomyosis model group; Group II, melatonin 10 mg/kg body weight (Me 10); Group III, melatonin 20 mg/kg body weight (Me 20); Group IV, melatonin 30 mg/kg body weight (Me 30); and Group V, melatonin 50 mg/kg body weight (Me 50). Melatonin (Sigma-Aldrich, St. Louis, MO, USA) was dissolved in a small volume (0.02 mL) of absolute ethanol and diluted in normal saline to a final concentration of 1 mg/mL. Mice from Groups II, III, IV, and V were intraperitoneally (i.p.) injected with melatonin every 12 h at various doses (5, 10, 15, and 25 mg/kg body weight) for 4 weeks, while those in the control and adenomyosis model groups followed the same regimen and received sham injections (without melatonin). During days 110–125, the estrous cycles of female mice were mated with fertile male mice from 19:00 to 07:00, then checked for the presence of a vaginal plug at 08:00–9:00 the following day. The vaginal plug day was defined as gestation day 0.5. Pregnant animals were killed by cervical dislocation on day 8.5 for implantation site count, and the optimal concentration of melatonin was determined by the number of implantation

sites and used for the subsequent study. In a second experiment, a different group of female mice received the same treatments as described, after which the animals were euthanized at gestation day 4.5 (implantation window) of pregnancy, the uterus was removed for morphometric and endometrial receptivity analyses, and the oviducts collected for blastocyst retrieval. In the parallel study, pups were born approximately 21 days after mating, and the pregnancy rate and number of offspring were recorded and statistically analyzed. Each group contained at least six mice. The detailed procedures are presented in *Figure 1A*.

Uterine section and morphometric analysis

Uterine tissues from the experimental mice were harvested at night on day 4.5, with approximately 4/5 fractions of the uterus used for collecting endometrial tissues. The remaining sections were formalin-fixed and paraffin-embedded, then used for hematoxylin and eosin (H&E) staining and immunohistochemical (IHC) and immunofluorescence (IF) analysis. Images of H&E and IHC were observed under a Motic EasyScanner (Motic China Group Co., Ltd., Xiamen, China) and photographed. Six sections from each uterus were analyzed, and morphometric parameters were measured using Image Pro-Plus software (v.6.0; Media Cybernetics, Silver Spring, MD, USA). The interface between the myometrial and endometrial layers (P1) and the inner luminal surface area (P2) was traced, and the latter was subtracted from the former as the endometrial area (EA). The endometrial thickness index (ETI) was used to determine the thickness of the endometrium, which was calculated using the formula: $ETI = 2EA/(P1 + P2)$ (25,26). Two investigators independently completed the measurement on different occasions.

RNA extraction and quantitative reverse transcription polymerase chain reaction (qRT-PCR)

Total RNA was extracted using TRIzol reagent (Invitrogen, Carlsbad, CA, USA). After the measurement of RNA concentration and quality, RNA was reverse transcribed to complementary DNA (cDNA) using a PrimeScript RT Reagent Kit (TaKaRa Bio, Shiga, Japan) according to the manufacturer's instructions. Primers were designed and purchased from Sangon Biotechnology (Shanghai, China). qRT-PCR was performed using a TB Green Premix Ex Taq kit (TaKaRa Bio) and an Applied Biosystems 7500 Fast Real-Time PCR System (Thermo Fisher Scientific,

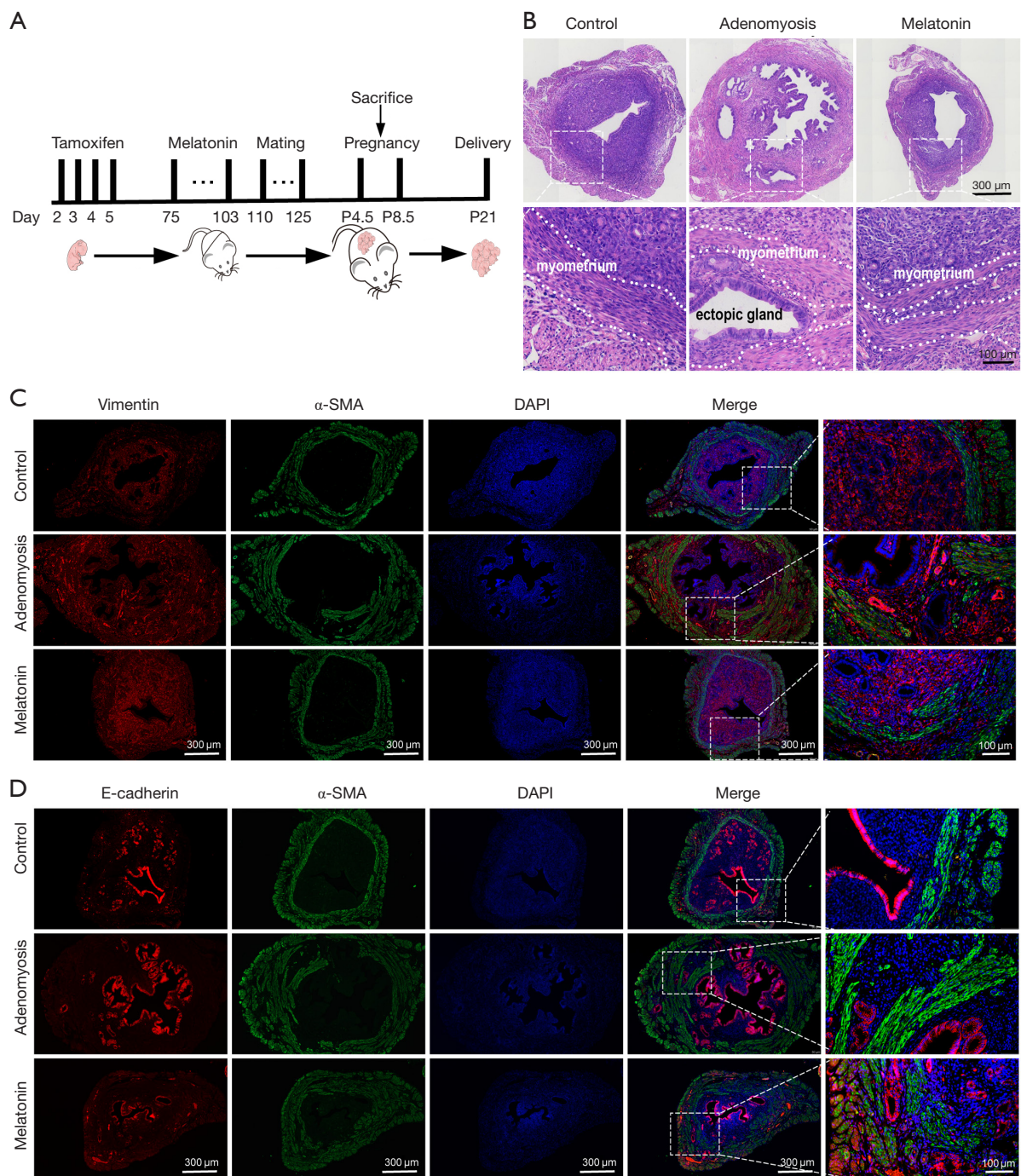


Figure 1 Construction and confirmation of adenomyosis mouse model. (A) Female neonatal CD-1 mice were orally dosed tamoxifen on days 2 through 5 after birth. After 75 days, tamoxifen-treated mice were injected with melatonin for 28 days. Estrous mice were then mated with fertile male mice and harvested at pregnancy 4.5 and 8.5, and the pregnancy rate and the number of litter size were recorded. (B) H&E staining showed the myometrium was disrupted and disordered in all tamoxifen-treated mice, and endometrial glands and stromal cells invaded the muscle layer in adenomyosis model mice (dotted line). (C,D) IF staining depicted myometrial disorders (α -SMA) with stroma (vimentin) and gland epithelium (E-cadherin) invade the muscle layer in all tamoxifen-treated mice ($n=9$). α -SMA, α -smooth muscle actin; DAPI, 4,6-diamidino-2-phenylindole; H&E, hematoxylin and eosin; IF, immunofluorescence.

Table 1 Primers for qRT-PCR

Genes	Primer sequence (5'-3')	Product size (bp)	T _m (°C)
<i>GAPDH</i>	Forward: AGGTCGGTGTGAACGGATTTG	123	60.88
	Reverse: TGTAGACCATGTAGTTGAGGTCA		58.59
<i>LIF</i>	Forward: GCTGTATCGGATGGTCGCATA	156	60.07
	Reverse: CACAGACGGCAAAGCACATT		59.69
<i>Integrin β3</i>	Forward: GCGGTTGTTGTTGGAGAGTC	138	59.41
	Reverse: CTTCAGGTTACATCGGGGTGA		59.45
<i>HoxA10</i>	Forward: GGCAGTTCCAAAGGCGAAAAT	86	60.00
	Reverse: GTCTGGTGCTTCGTGAAGGG		60.94
<i>HoxA11</i>	Forward: ATAGCACGGTGGGCAGGAACG	96	65.06
	Reverse: AGTCGGAGGAAGCGAGGTTTT		61.71
<i>Era</i>	Forward: TGTCAGCAGTAACGAGAAAGG	94	60.29
	Reverse: TGGTAGCCAGAGGCATAGTCAT		60.69
<i>Pra</i>	Forward: CTCCGGGACCGAACAGAGT	128	60.98
	Reverse: GCGGGGACAACAACCCTTT		60.83
<i>P53</i>	Forward: TGAGGTTTCGTGTTTGTGCCTGC	165	64.06
	Reverse: CCATCAAGTGGTTTTTCTTTTGC		58.19
<i>Gpx1</i>	Forward: CCACCGTGTATGCCTTCTCC	105	60.46
	Reverse: AGAGAGACGCGACATTCTCAAT		59.57
<i>Sod1</i>	Forward: CACTCTCAGGAGAGCATTCCA	110	59.17
	Reverse: CCCAGCATTTCAGTCTTTG		56.98
<i>Bcl-2</i>	Forward: ACCTGTGGTCCATCTGACCCTC	163	63.42
	Reverse: CCAGTTCACCCCATCCCTGA		61.21
<i>Bax</i>	Forward: AGACAGGGGCTTTTTGCTAC	137	60.55
	Reverse: AATTCGCCGAGACACTCG		60.15

qRT-PCR, quantitative reverse transcription polymerase chain reaction; GAPDH, glyceraldehyde 3-phosphate dehydrogenase; LIF, leukemia inhibitory factor; HoxA10, homeobox A10; HoxA11, homeobox A11.

Waltham, MA, USA) according to the manufacturer's instructions. Glyceraldehyde 3-phosphate dehydrogenase (*GAPDH*) was used as the standard control, and primer sequences are listed in *Table 1*. Relative quantification of gene expression was performed using the $2^{-\Delta\Delta CT}$ method.

Western blot

Protein concentrations were determined using a BCA protein assay kit (Thermo Fisher Scientific). Equal amounts of total protein (30 μg/lane) were loaded and separated by sodium dodecyl sulfate-polyacrylamide gel electrophoresis,

then transferred onto polyvinylidene difluoride membranes (EMD Millipore, Burlington, MA, USA) according to standard procedures. The membranes were then blocked using 5% non-fat milk (Sangon Biotechnology) in Tris-buffered saline with 0.05% Tween-20 detergent for 1.5 h on a shaker then incubated with primary antibody against GAPDH (1:1,000; #5174; Cell Signaling Technology, Boston, MA, USA), LIF (1:1,000; DF13730; Affinity, Changzhou, China), integrin β3 (1:1,000; AF6086; Affinity), HoxA10 (1:1,000; #58891; Cell Signaling Technology), HoxA11 (1:1,000; ab72591; Abcam, Cambridge, UK), phospho-p44/42 MAPK (Erk1/2) (Thr202/Tyr204)

(1:2,000; #4370; Cell Signaling Technology), p44/42 MAPK (Erk1/2) (1:1,000; #9102; Cell Signaling Technology), phospho-p38 MAPK (Thr180/Tyr182) (1:1,500; T40076; Abmart, Shanghai, China), p38 MAPK (1:1,500; T55600; Abmart), TNF- α (1:500; AF7014; Affinity), IL-1 β (1:1,000; AF5103; Affinity), p-NF- κ B p65 (Ser536) (1:1,500; TA2006; Abmart), NF- κ B p65 (1:1,500; TA5006; Abmart), Bax (1:1,000; T40051; Abmart), Bcl-2 (1:1,000; T40056; Abmart), cleaved caspase-3 (1:1,000; #9664; Cell Signaling Technology), caspase-3 (1:1,000; #9662; Cell Signaling Technology), and vascular endothelial growth factor (VEGF) (1:500; 19003-1-AP; Proteintech, Chicago, IL, USA) at 4 °C overnight, incubation with horseradish peroxidase-conjugated anti-rabbit immunoglobulin G (IgG) secondary antibodies at room temperature for 1.5 h followed. Images were obtained using a chemiluminescent imaging system (Tanon Science & Technology Co., Ltd., Shanghai, China), with GAPDH used as the internal control. The intensities of the protein bands were quantified using Image J software (National Institutes of Health, Bethesda, MD, USA).

Immunohistochemistry

Formalin-fixed, paraffin-embedded uteri were subjected to routine 5 μ m thickness sectioning for IHC analysis, and all IHC experiments were performed using a standard protocol. Briefly, sections were deparaffinized by incubating with xylene for 30 mins and rehydrated in an ethanol series, followed by antigen retrieval and endogenous peroxidase blockage. Sections were then incubated with respective primary antibodies, including anti-LIF (1:50; DF13730; Affinity), integrin β 3 (1:50; AF6086; Affinity), HoxA10 (1:50; #58891; Cell Signaling Technology), and HoxA11 (1:50; ab72591; Abcam), overnight at 4 °C in a humidified chamber, followed by incubation with the corresponding secondary antibodies. Phosphate-buffered saline was used as the negative control instead of the primary antibody. Image Pro-Plus software (v.6.0; Media Cybernetics) was used to evaluate the reactivity of the endometrial glands and luminal surface epithelium of the uterus (average positively-stained area percentage) using two independent analyzers.

IF

Paraffin sections (3 μ m) were routinely subjected to deparaffinization and rehydration with xylene and descending concentrations of alcohol, and permeabilized

with 1% Triton X-100 for 10 min. After endogenous peroxidases blocking and serum blocking, the sections were incubated with vimentin antibody (1:200; #5741; Cell Signaling Technology)/E-cadherin antibody (1:200; #3195; Cell Signaling Technology)/ α -smooth muscle actin (α -SMA) antibody (1:200; NB300-978; Novus, Centennial, CO, USA) at 4 °C overnight. Sections were then rinsed with phosphate-buffered saline with Tween 20 (PBST) and incubated with donkey anti-rabbit secondary antibody (1:500; Invitrogen)/donkey anti-goat secondary antibody (1:500; Invitrogen) for 60 min at room temperature. The cells were ultimately washed with PBST and stained with 4,6-diamidino-2-phenylindole (DAPI) (Beyotime, Shanghai, China) to visualize nuclei, and analyzed with a Leica microscope (Leica, Wetzlar, Germany).

Statistics analysis

All experiments were conducted at least three times, and data are represented as mean \pm standard deviation (SD). Statistical analyses were conducted using one-way analysis of variance, followed by Turkey's or Bonferroni post hoc analysis for multiple comparisons. All analyses were performed using GraphPad Prime software (GraphPad Software, LaJolla, CA, USA) and SPSS (v.18.0; SPSS Inc., Chicago, IL, USA). $P < 0.05$ was considered statistically significant.

Results

Artificial induction of adenomyosis mouse model

We established an adenomyosis mouse model to explore the role of melatonin on uterine receptivity in adenomyosis. A total of 96 mice were used for the first experiment, and H&E pathology and IF analyses were used to verify the effectiveness of the model ($n=9$). As shown in *Figure 1B*, the circular muscle layer was well developed to form an intact ring structure in control mice. However, the endometrial glands and stromal cells invaded the muscle layer, resulting in the distorted and disrupted myometrium in all tamoxifen treated mice. IF analysis of vimentin or E-cadherin co-staining with α -SMA also clearly demonstrated that endometrial epithelial and stroma cells invaded the disordered muscle layer (*Figure 1C, 1D*). These results indicated neonatal mice treated with tamoxifen represented a successful method for modeling adenomyosis.

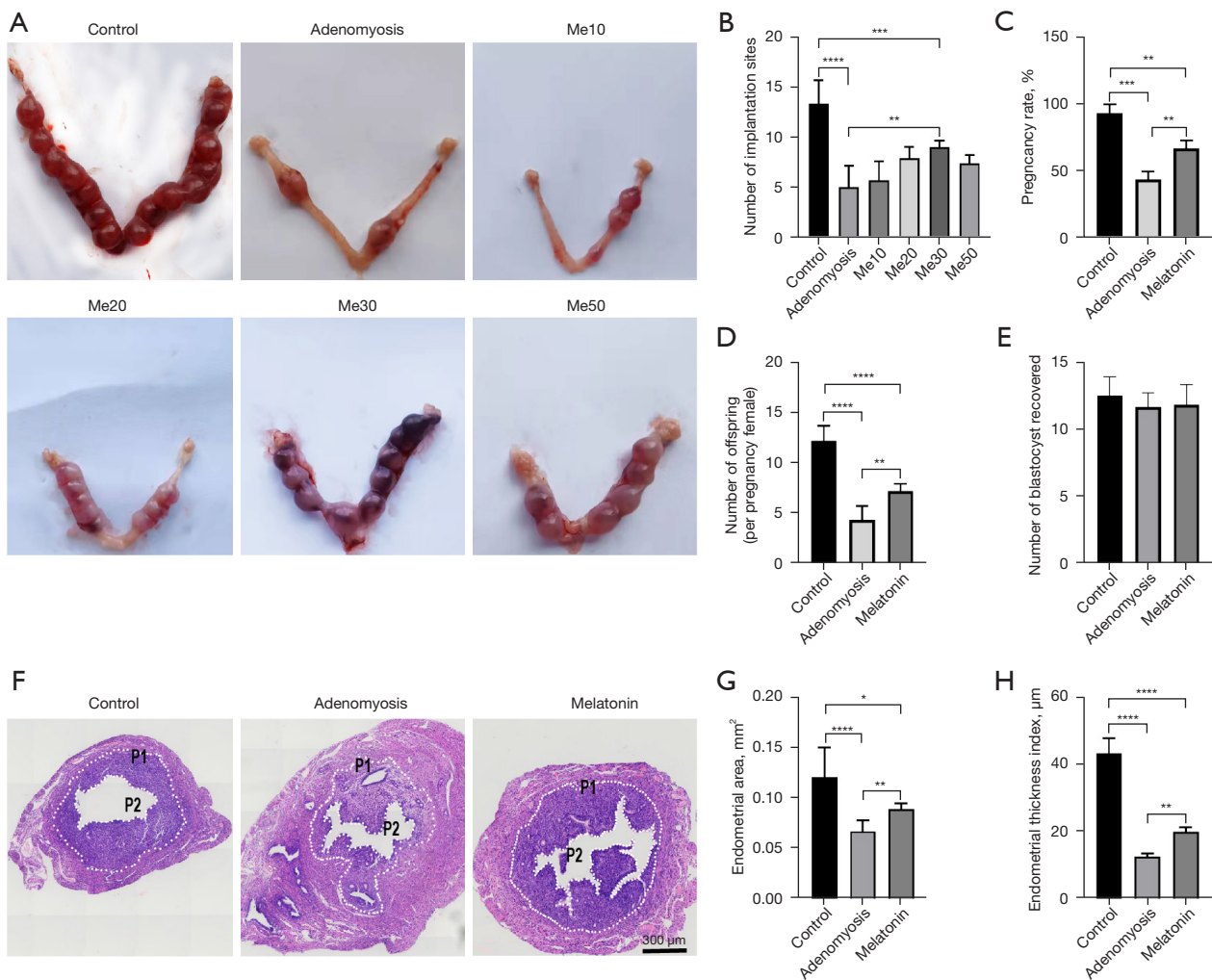


Figure 2 Effect of melatonin on the number of implantation sites, pregnancy outcomes, and endometrial development. (A,B) Number of implantation sites, (C) pregnancy rate, (D) number of offspring, and (E) recovered blastocysts. (F) H&E sections showed abnormal endometrial morphology in mice treated with tamoxifen and that abnormal endometrial development was significantly improved after melatonin injection. (G) The lower EA and (H) ETI caused by tamoxifen were significantly ameliorated after melatonin treatment. **** $P < 0.0001$; *** $P < 0.001$; ** $P < 0.01$; * $P < 0.05$; $n = 6$. Me10, melatonin 10 mg/kg body weight; Me20, melatonin 20 mg/kg body weight; Me30, melatonin 30 mg/kg body weight; Me50, melatonin 50 mg/kg body weight; P1, the myometrial and endometrial layers; P2, the inner luminal surface area; H&E, hematoxylin and eosin; EA, endometrial area; ETI, endometrial thickness index.

Melatonin improves pregnancy outcomes and endometrial development of adenomyosis model mice

To clarify whether melatonin improved pregnancy outcomes in adenomyosis model mice, we analyzed the implantation sites in the different treatment groups. As shown in *Figure 2A,2B*, the number of implantation sites in the adenomyosis model mice was much less than in control mice (5.0 ± 2.10 vs. 13.3 ± 2.38 , $P < 0.0001$, $n = 6$). However, after long-term melatonin injection (28 days), a downward

trend of implantation sites caused by adenomyosis was ameliorated. In particular, 30 mg/kg melatonin therapy significantly increased the number of implantation sites (9.0 ± 0.63 vs. 5.0 ± 2.10 , $P = 0.002$, $n = 6$). Therefore, we determined 30 mg/kg of melatonin as the optimal concentration for subsequent studies.

To determine whether melatonin improved pregnancy outcomes in mice with adenomyosis, we mated estrous females to fertile male mice, and as shown in *Figure 2C,2D*,

the pregnancy rate and average litter size were significantly reduced in the adenomyosis group (n=6). However, the low pregnancy rate and reduced offspring caused by adenomyosis were significantly ameliorated in the melatonin treatment group, suggesting melatonin may restore fertility in tamoxifen-exposed mice.

To clarify whether the treatments affected ovulation, blastocysts were flushed from uteri at day 4.5 (n=6), revealing no differences among the three groups (Figure 2E).

To elucidate the mechanism, endometrial development was analyzed (n=6), and uterine morphology analyses showed treatment with tamoxifen caused abnormal endometrial morphology which was significantly relieved when treatment was combined with melatonin (Figure 2F). Furthermore, we measured the EA and ETI, and as shown in Figure 2G,2H, the lower EA and ETI caused by tamoxifen were significantly ameliorated in the melatonin therapy group (P<0.01). This suggested melatonin could restore the damaged endometrial development in adenomyosis mice.

Melatonin reversed impaired endometrial receptivity caused by adenomyosis

To explore the mechanism of the beneficial effect of melatonin on implantation, the gene and protein expression of implantation-related markers in the endometrium of uteri during the window of implantation (n=6) were measured. The results showed endometrial receptivity related genes deteriorated in the adenomyosis model group, with adenomyotic endometrium showing significant decreases in *LIF*, *integrin β3*, *HoxA10*, and *HoxA11* messenger RNA (mRNA) levels relative to those in control mice. However, their levels were significantly upregulated after melatonin treatment (Figure 3A), and the protein levels were consistent with their gene expressions (Figure 3B,3C).

Furthermore, IHC staining revealed LIF and integrin β3 were mainly located in the cytoplasm of endometrial luminal epithelial cells and glandular epithelial cells, whereas *HoxA10* and *HoxA11* were expressed in the nuclei of endometrial luminal epithelial cells and glandular epithelial cells (Figure 3D). Quantitative analysis of IHC data revealed levels of LIF, integrin β3, *HoxA10*, and *HoxA11* were significantly lower in adenomyosis mice than in the control group, and importantly, melatonin treatment significantly recovered these markers (Figure 3E). Taken together, these results suggested melatonin ameliorated the damaged endometrial receptivity caused by adenomyosis.

Melatonin alleviates aberrant endometrial metabolism

To further explore the potential mechanism of the beneficial effects of melatonin on endometrial receptivity, we extracted mRNA from the eutopic endometrium of mice and determined changes in the expression of implantation-related (*Era*, *Pra*, and *P53*), oxidative-stress-related (*Sod1* and *Gpx1*), and apoptosis-related (*Bcl-2* and *Bax*) genes by qRT-PCR (n=6). The results showed significantly lower *Era* expression in the adenomyosis model group compared with the control and melatonin-treated mice (Figure 4A), whereas *Pra* expression remained unchanged (Figure 4B), and *P53* expression was significantly upregulated (Figure 4C). Oxidative stress was considered an important factor affecting the female reproductive system, and melatonin was reportedly involved in redox homeostasis (27). In the present study, we found adenomyosis altered the expression of oxidative-stress-related genes, whereas melatonin treatment ameliorated oxidative stress by significantly decreasing the expression of *Gpx1* (Figure 4D) and upregulating the expression of *Sod1* (Figure 4E). Excessive oxidative stress often leads to apoptosis. Although there was no difference between pro-apoptotic gene *Bax* (Figure 4F), expression of the anti-apoptotic gene *Bcl-2* was lower and the ratio of *Bax/Bcl-2* was higher in adenomyosis model mice than in the other two groups, whereas melatonin treatment markedly upregulated *Bcl-2* and downregulated the ratio of *Bax/Bcl-2* expression relative to the untreated model group (Figure 4G,4H).

Excessive oxidative stress and inflammatory factors not only damage the embryo, but also reduced the function of endometrium. To further elucidate the mechanism of melatonin's effect, we detected the expression of apoptotic-associated proteins in the endometrium. The results of Western blot analysis (Figure 5A,5B) show that compared with control mice, adenomyosis mice had higher expression of cleaved caspase-3, caspase-3, the ratio of cleaved caspase-3/caspase-3 and *Bax/Bcl-2*, and after melatonin treatment these decreased significantly. In addition, although *Bcl-2* expression did not change significantly, the trend of *Bax* increased in the adenomyosis group.

To further explore the protective effect of melatonin, the VEGF expression was also examined. The results of Western blot showed that compared with the control group, the endometrium of the adenomyosis model mice during the implantation state had significantly decreased VEGF expression (Figure 5C,5D), and melatonin significantly increased VEGF expression. These results indicated

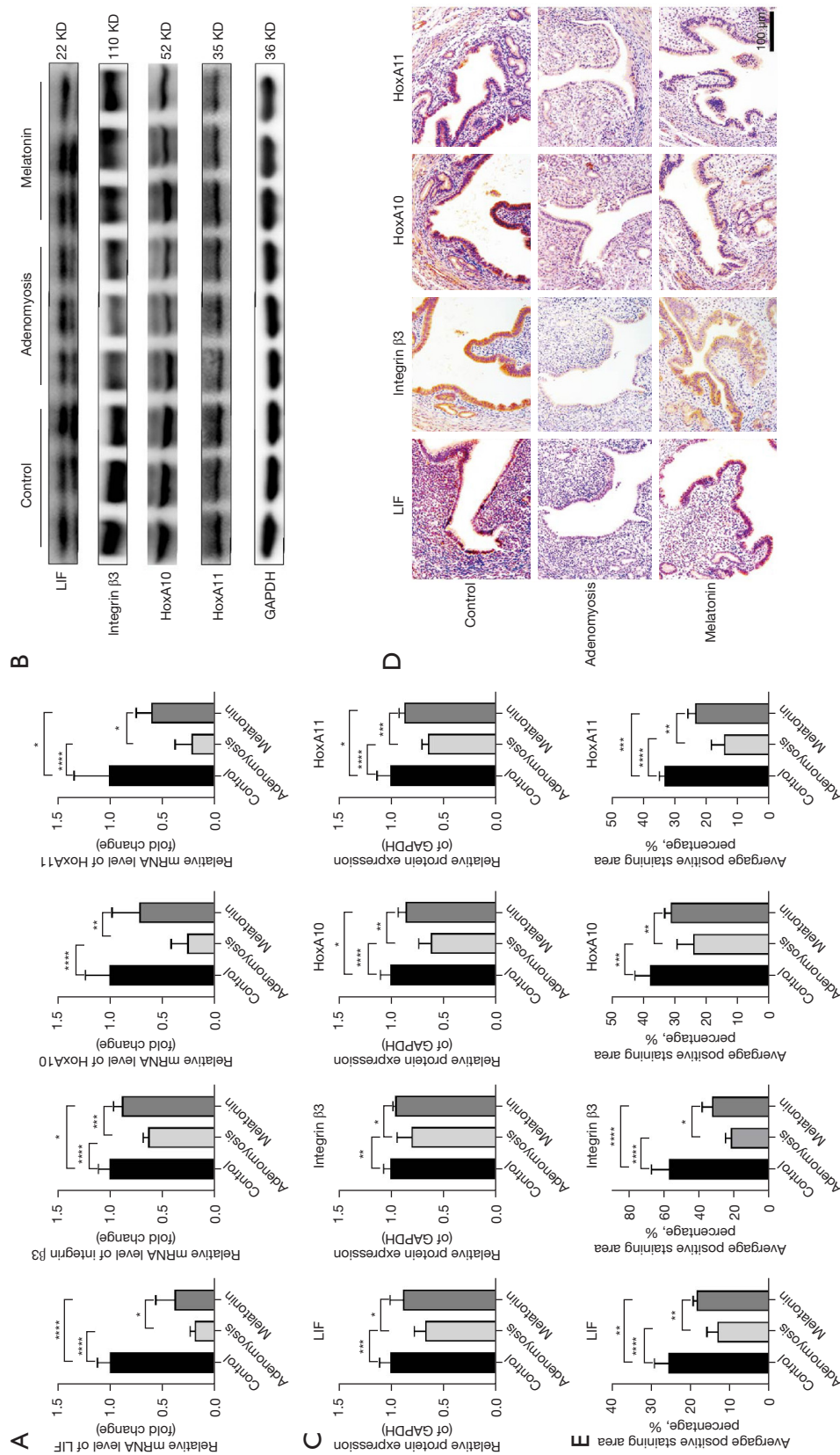


Figure 3 Melatonin administration improved endometrial receptivity during the implantation state. (A) Effects of melatonin on mRNA levels of endometrial receptivity markers (*LIF*, *integrin $\beta 3$* , *HoxA10*, and *HoxA11*) by qRT-PCR in endometrium during the window of implantation between the control, adenomyosis model, and melatonin treated mice. (B) Western blot gels of *LIF*, *integrin $\beta 3$* , *HoxA10*, and *HoxA11*. (C) Bar graph showing the quantification of *LIF*/*GAPDH*, *integrin $\beta 3$* /*GAPDH*, *HoxA10*/*GAPDH*, and *HoxA11*/*GAPDH*, respectively. (D) Images of immunohistochemistry for *LIF*, *integrin $\beta 3$* , *HoxA10*, and *HoxA11*, and (E) corresponding quantified expression values. **** $P < 0.0001$; *** $P < 0.001$; ** $P < 0.01$; * $P < 0.05$; n=6. mRNA, messenger RNA; LIF, leukemia inhibitory factor; HoxA10, homeobox A10; HoxA11, homeobox A11; GAPDH, glyceraldehyde 3-phosphate dehydrogenase; qRT-PCR, quantitative reverse transcription polymerase chain reaction.

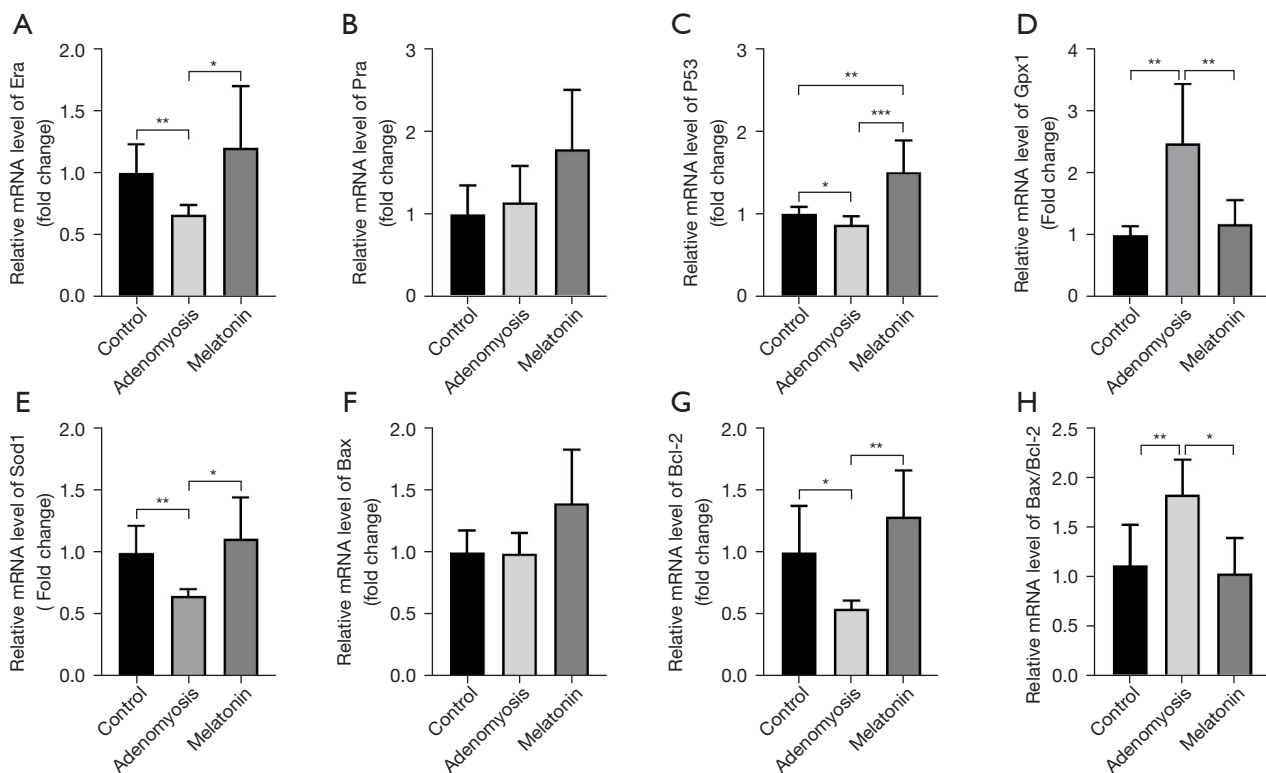


Figure 4 Effects of melatonin on the implantation-related, antioxidative-associated, and apoptosis gene expression. (A-C) mRNA expression of implantation-related genes *Era*, *Pra*, and *P53*, (D,E) antioxidative-associated genes *Gpx1* and *Sod1*, (F-H) apoptosis-correlated genes of *Bax*, *Bcl-2*, and the ratio of *Bax/Bcl-2* in endometrium during implantation state from mice of the control, adenomyosis model, and melatonin treated groups. *** $P < 0.001$; ** $P < 0.01$; * $P < 0.05$; $n = 6$. mRNA, messenger RNA.

melatonin could exert a protective effect against oxidative stress induced by adenomyosis and reduce endometrial apoptosis to improve endometrial receptivity.

Melatonin reduces abnormal inflammatory responses in adenomyosis mice by suppressing NF- κ B signaling

To investigate the underlying molecular mechanisms of melatonin in adenomyosis model mice, we first investigated changes in levels of the proinflammatory cytokines TNF- α and IL-1 β in the endometrium during the implantation window ($n = 6$). Western blot analysis showed adenomyosis model mice had higher TNF- α and IL-1 β levels compared with control mice (Figure 6A,6B). A previous study reported melatonin exerted an anti-inflammatory effect during disease treatment (28). Therefore, we examined whether it inhibited the release of proinflammatory cytokines in the endometrium of mice with adenomyosis, with the results confirming it significantly reduced TNF- α and IL-1 β levels

(Figure 6A,6B). NF- κ B and MAPK signaling pathways were involved in melatonin-regulated cell functions (20,29), and in the present study, we determined the relative contributions of p-NF- κ B p65, NF- κ B p65, phospho-p44/42 MAPK, p44/42 MAPK, phospho-p38 MAPK and p38 MAPK in melatonin-mediated suppression of TNF- α and IL-1 β production in endometrial tissue at day 4.5 ($n = 6$). However, Western blot results revealed no differences in levels of phospho-p44/42 MAPK, p44/42 MAPK, Phospho-p38 MAPK and p38 MAPK among the three groups (Figure 6C,6D), suggesting melatonin treatment reduced the secretion of proinflammatory cytokines in adenomyosis, although not via the p44/42 MAPK and p38 MAPK signaling pathways.

NF- κ B activation was also enhanced by TNF- α stimulation, and according to the feed-forward relationship between proinflammatory factors and NF- κ B activation, it was likely activated NF- κ B might result in increased production of proinflammatory chemokines (13).

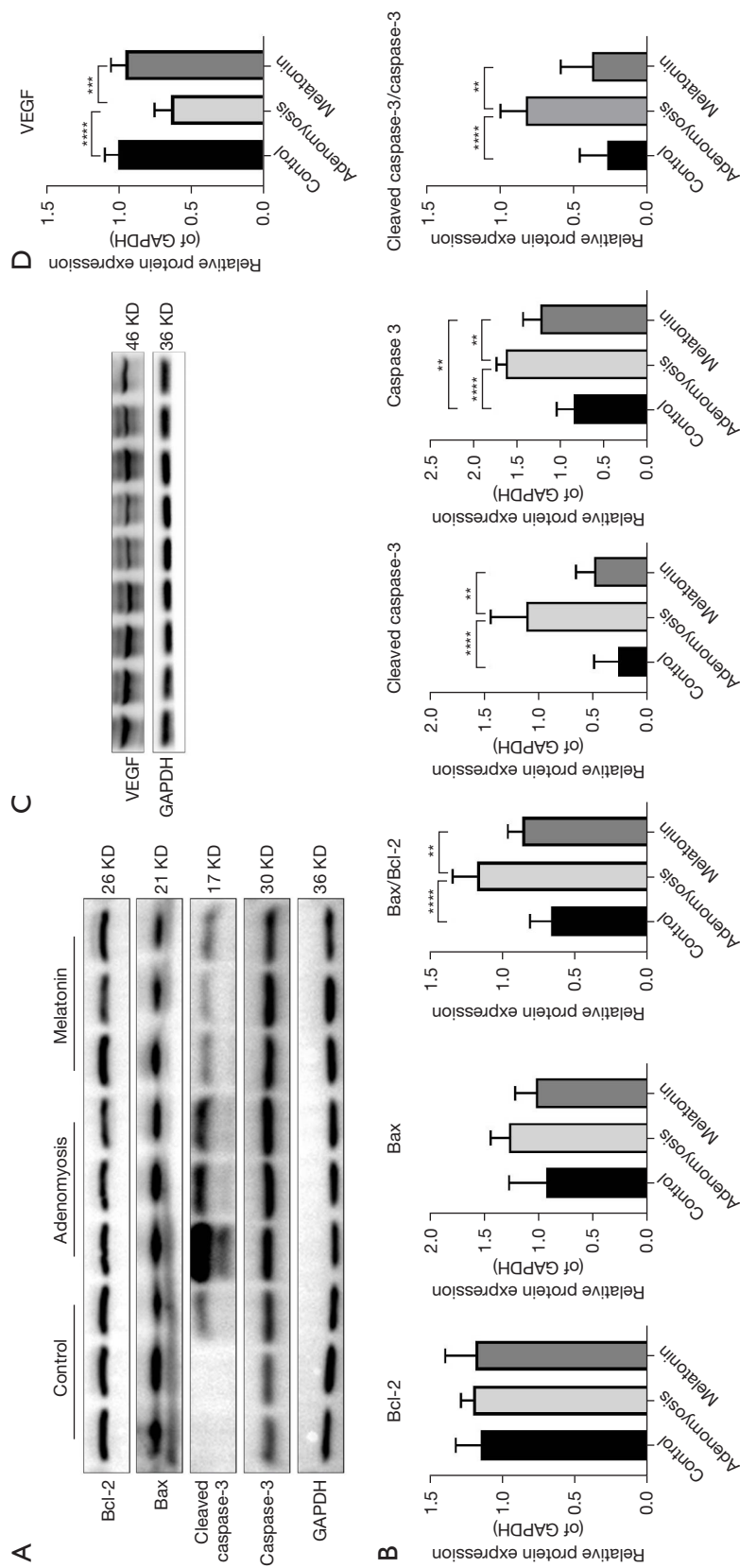


Figure 5 Melatonin reduced endometrial cell apoptosis and improved the expression of VEGF. (A) Expression of apoptosis-related proteins of Bcl-2, Bax, cleaved caspase-3, and caspase-3 in mouse endometrium among control, adenomyosis model, and melatonin treatment groups. (B) Apoptosis-related protein levels were normalized to GAPDH in the Western blot analysis. (C,D) VEGF protein levels in control, adenomyosis model, and melatonin injection mice. **** $P < 0.0001$; *** $P < 0.001$; ** $P < 0.01$; n=6. GAPDH, glyceraldehyde 3-phosphate dehydrogenase; VEGF, vascular endothelial growth factor.

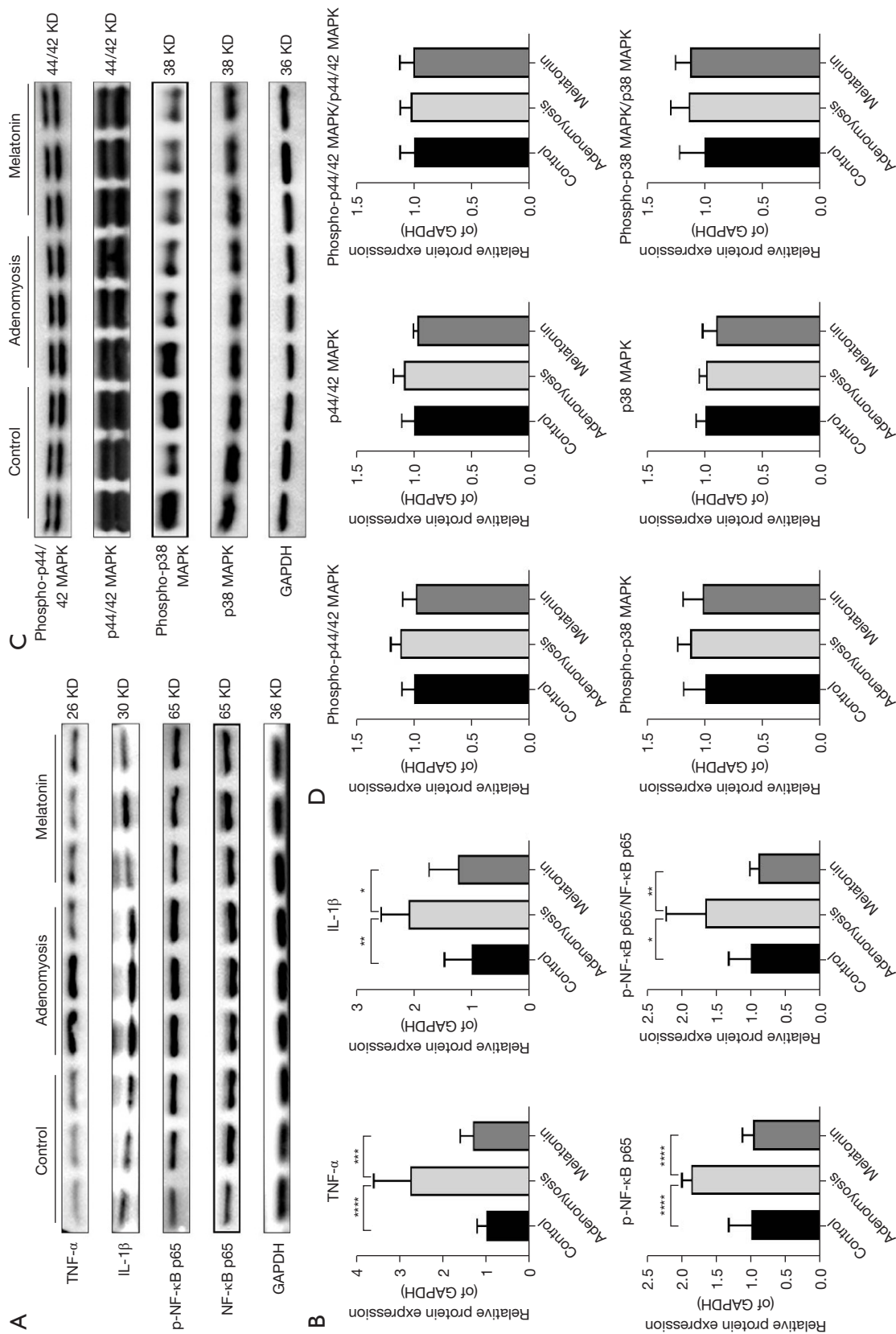


Figure 6 Melatonin inhibits the expression of inflammatory factors in an adenomyosis model mice via the NF- κ B signaling pathway. (A) Representative Western blotting images of inflammation-related proteins of TNF- α , IL-1 β , p-NF- κ B p65, and NF- κ B p65 in the endometrium of control, adenomyosis model and melatonin treated groups during the implantation window. (B) Bar graph showing the quantification of TNF- α /GAPDH, IL-1 β /GAPDH, p-NF- κ B p65/GAPDH and the ratio of p-NF- κ B p65/NF- κ B p65 respectively. (C) Western blot detection of phospho-p44/42 MAPK, p44/42 MAPK, p38 MAPK, and melatonin treated groups. (D) Quantitative analysis of phospho-p44/42 MAPK, p44/42 MAPK, p38 MAPK, and the phospho-p38 MAPK/phospho-p38 MAPK ratio normalized against GAPDH. ****P<0.0001; ***P<0.001; **P<0.01; *P<0.05; n=6. TNF- α , tumor necrosis factor- α ; IL-1 β , interleukin-1 β ; NF- κ B, nuclear factor kappa B; GAPDH, glyceraldehyde 3-phosphate dehydrogenase.

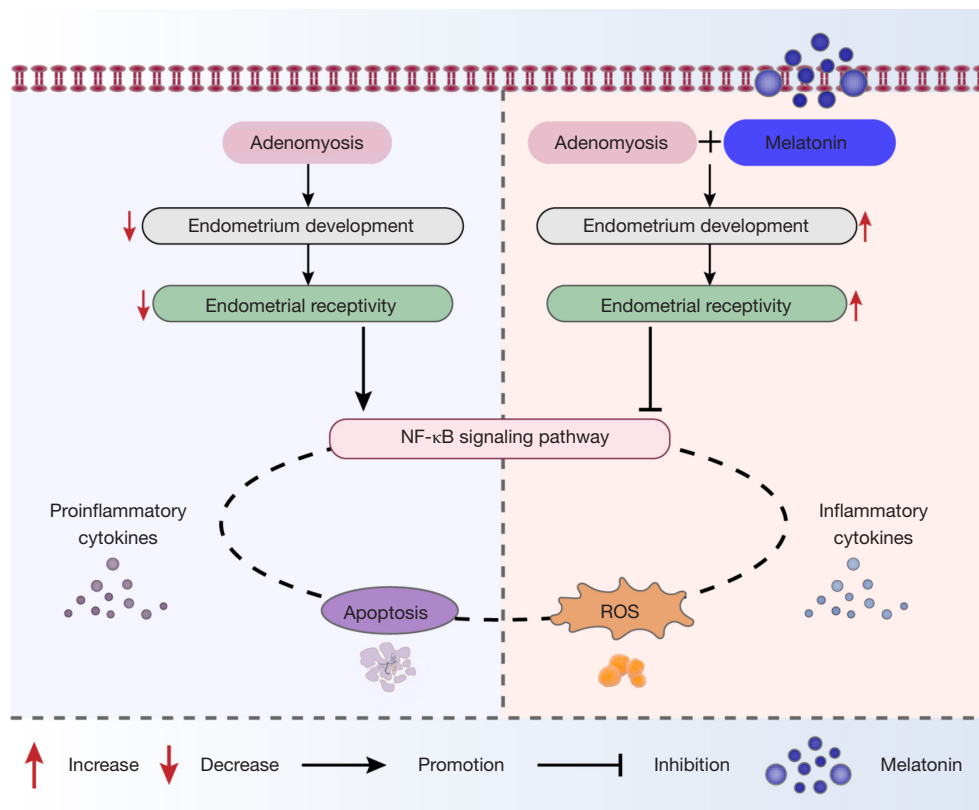


Figure 7 Schematic diagram of the regulatory mechanism of melatonin in the adenomyosis model mice. NF- κ B, nuclear factor kappa B; ROS, reactive oxygen species.

Interestingly, as shown in *Figure 6A,6B*, adenomyosis induced higher levels of p-NF- κ B p65 and the p-NF- κ B p65/NF- κ B p65 ratio than those observed in control mice, whereas melatonin administration significantly reduced both. These data suggested NF- κ B may play a pivotal role in the development of adenomyosis by promoting inflammation and excessive oxidative stress, and further impairing endometrial development. Furthermore, the results indicated melatonin might reduce TNF- α and IL-1 β production in the endometrium of adenomyosis mice, suppressing the NF- κ B signaling (*Figure 7*).

Discussion

Adenomyosis is a common disease in women of reproductive age, manifesting a variable degree of symptoms while causing reproductive failure in a high percentage of patients (4). Adjuvant measures to improve pregnancy outcomes have been extensively explored, but the results are not satisfactory. In the present study, we showed adenomyosis

had a detrimental effect on uterine receptivity in mice, and melatonin therapy significantly reversed this by reducing the inflammatory reaction, oxidative stress, and apoptosis by suppressing the NF- κ B signaling pathway.

The endometrium is the primary target organ for embryo implantation, and its development state is directly related to embryo survival and implantation, and the establishment and maintenance of gestation (30). The correlation between endometrial thickness (Eth) and the ability of embryos to implant has been analyzed, and there is a general consensus that a higher Eth results in a better chance of implantation (31). Additionally, Eth is closely related to EA. In the present study, we found endometrial morphology developed more poorly in adenomyosis model mice than in control mice. We observed a “thin” endometrium which was likely the morphologic expression of defective vascularization during the invasive phase. However, this morphology improved following melatonin administration but had no effect on ovulation, which indirectly indicated melatonin replacement may effectively restore normal

physiological function of the endometrium. In females, estradiol (E_2) and progesterone play crucial roles in multiple reproductive systems, and their functions are mediated by the nuclear receptors *Era* and *Pra*. During pre-implantation, a small surge of E_2 is critical for inducing mouse uterine receptivity. Blastocysts can locally synthesize and secrete E_2 to initiate implantation (32), and the knockout of nuclear estrogen and progesterone receptors leads to complete infertility (33,34). In our study, we observed reduced *Era* expression on day 4.5 in adenomyosis model mice, and exogenous melatonin supplementation actively upregulated this expression to sensitize the uterus, although no change was observed in *Pra* expression. The same trend was observed in *P53* expression, a gene critical for implantation. This may be because low local estrogen levels in the endometrium dysregulated matrix remodeling during the implantation window, leading to poor endometrial development and further damaging embryo implantation.

In adenomyosis mice, higher local levels of ROS and inflammatory cytokines in the uterus induced cell apoptosis and tissue damage, changed the uterine microenvironment, affected embryo implantation, and reduced fertility. As shown in *Figure 3*, the expression of LIF, integrin $\beta 3$, HoxA10, and HoxA11 showed an obvious trend of decline. During embryo implantation, weak gene expression changes in LIF, integrin $\beta 3$, HoxA10, and HoxA11 regulated some implantation-related genes and signaling pathways. Therefore, we believed the imbalance of immune regulation of endometrial cells induced by adenomyosis was an important factor leading to the decline of endometrial receptivity.

Melatonin benefits reproductive physiology as a free radical scavenger and upregulates the expression of antioxidant- or apoptosis-related genes (35,36). When ROS reach a maximum resistance threshold, tissue damage or even cell death can occur. Here, we found a dramatic decrease in *Sod1* mRNA levels in adenomyosis model mice, but these were upregulated following melatonin treatment. Notably, *Gpx1* expression was highest, which may be due to the necessity for high levels of *Gpx1* to remove excessive peroxide ions in the endometrium. Excessive oxidative stress often leads to apoptosis, which is an important regulator of eutopic endometrial function. Contrary to earlier reports in the rat, the genes expression of anti-oxidative genes (*SOD1*, *Gpx1*) and apoptosis-associated genes (*caspase-3*, *Bcl-2*) were not changed after melatonin treatment (23).

The pathogenesis of adenomyosis-associated subfertility has not been fully elucidated and was the focus of the

present study. The abnormal microenvironment of the endometrium in adenomyosis model mice stimulated endometrial cells to produce inflammatory damage, which might activate NF- κ B signaling. NF- κ B transferred from the cytoplasm to the nucleus, initiated the transduction of multiple downstream inflammatory signal pathways, released inflammatory factors such as TNF- α and IL-1 β , participated in a series of immune responses, caused a localized hyperinflammatory response, produced obvious toxic effects on embryos and endometrial epithelium, and reduced the implantation rate (37). Our results showed melatonin decreased the ROS level and apoptosis induced by adenomyosis, increased VEGF expression, and improved pregnancy outcomes, providing new insight into melatonin-based therapy for adenomyosis infertility.

There are some limitations in our study. Firstly, as the process of embryo implantation is a complex regulatory network and we only examined endometrium development, further experiments are needed to systematically study the interaction between embryo and receptive endometrium. Moreover, the pathway inhibitor of NF- κ B was required to clarify the mechanism of melatonin.

Conclusions

In summary, adenomyosis induced endometrial cell apoptosis during window of implantation by activating the Bax/caspase-3 mitochondrial apoptosis pathway through ROS and caused an inflammatory response through the NF- κ B pathway in adenomyosis mice. Melatonin alleviated apoptosis by inhibiting ROS, reducing TNF- α and IL-1 β expression and enhancing VEGF expression by inhibiting the NF- κ B signal pathway. These results demonstrate the protective effect of melatonin on adenomyosis, especially the positive melatonin-specific effects on uterine development and endometrial receptivity, and highlight its potential as an auxiliary therapeutic candidate for the treatment of fertility in adenomyosis patients.

Acknowledgments

The authors thank Dr. Qizhi He (Department of Pathology, Shanghai First Maternity and Infant Hospital, School of Medicine, Tongji University, Shanghai, China) and Song Guo (Gynecology Department, The First Affiliated Hospital of Shandong First Medical University, Jinan, China) for advice on establishment of the mouse model.

Funding: This work was supported by the Natural Science

Foundation of Shanghai, China (No. 21ZR1450700).

Footnote

Reporting Checklist: The authors have completed the ARRIVE reporting checklist. Available at <https://atm.amegroups.com/article/view/10.21037/atm-22-5493/rc>

Data Sharing Statement: Available at <https://atm.amegroups.com/article/view/10.21037/atm-22-5493/dss>

Conflicts of Interest: All authors have completed the ICMJE uniform disclosure form (available at <https://atm.amegroups.com/article/view/10.21037/atm-22-5493/coif>). The authors have no conflicts of interest to declare.

Ethical Statement: The authors are accountable for all aspects of the work in ensuring that questions related to the accuracy or integrity of any part of the work are appropriately investigated and resolved. Animal experiments in this study were approved by the Animal Ethics Committee of Tongji University (No. TJBG01321101) and conducted under the guidelines of the National Research Council's Guide for the Care and Use of Laboratory Animals.

Open Access Statement: This is an Open Access article distributed in accordance with the Creative Commons Attribution-NonCommercial-NoDerivs 4.0 International License (CC BY-NC-ND 4.0), which permits the non-commercial replication and distribution of the article with the strict proviso that no changes or edits are made and the original work is properly cited (including links to both the formal publication through the relevant DOI and the license). See: <https://creativecommons.org/licenses/by-nc-nd/4.0/>.

References

- Naftalin J, Hoo W, Pateman K, et al. Is adenomyosis associated with menorrhagia? *Hum Reprod* 2014;29:473-9.
- Chapron C, Vannuccini S, Santulli P, et al. Diagnosing adenomyosis: an integrated clinical and imaging approach. *Hum Reprod Update* 2020;26:392-411.
- Kunz G, Beil D, Huppert P, et al. Adenomyosis in endometriosis--prevalence and impact on fertility. Evidence from magnetic resonance imaging. *Hum Reprod* 2005;20:2309-16.
- Horton J, Sterrenburg M, Lane S, et al. Reproductive, obstetric, and perinatal outcomes of women with adenomyosis and endometriosis: a systematic review and meta-analysis. *Hum Reprod Update* 2019;25:592-632.
- Vercellini P, Consonni D, Dridi D, et al. Uterine adenomyosis and in vitro fertilization outcome: a systematic review and meta-analysis. *Hum Reprod* 2014;29:964-77.
- Younes G, Tulandi T. Effects of adenomyosis on in vitro fertilization treatment outcomes: a meta-analysis. *Fertil Steril* 2017;108:483-90.e3.
- Munro MG. Uterine polyps, adenomyosis, leiomyomas, and endometrial receptivity. *Fertil Steril* 2019;111:629-40.
- Crha Karel, Jeřeta Michal, Pilka Radovan, et al. Adenomyosis - its possible effect on endometrial function and receptivity. *Ceska Gynekol* 2021;86:205-9.
- Bulun SE, Yildiz S, Adli M, et al. Adenomyosis pathogenesis: insights from next-generation sequencing. *Hum Reprod Update* 2021;27:1086-97.
- Feng T, Wei S, Wang Y, et al. Rhein ameliorates adenomyosis by inhibiting NF- κ B and β -Catenin signaling pathway. *Biomed Pharmacother* 2017;94:231-7.
- Prince PD, Fischerman L, Toblli JE, et al. LPS-induced renal inflammation is prevented by (-)-epicatechin in rats. *Redox Biol* 2017;11:342-9.
- Yen CF, Liao SK, Huang SJ, et al. Decreased Endometrial Expression of Leukemia Inhibitory Factor Receptor Disrupts the STAT3 Signaling in Adenomyosis During the Implantation Window. *Reprod Sci* 2017;24:1176-86.
- Li B, Chen M, Liu X, et al. Constitutive and tumor necrosis factor- α -induced activation of nuclear factor- κ B in adenomyosis and its inhibition by andrographolide. *Fertil Steril* 2013;100:568-77.
- Carrarelli P, Yen CF, Funghi L, et al. Expression of Inflammatory and Neurogenic Mediators in Adenomyosis. *Reprod Sci* 2017;24:369-75.
- Zhihong N, Yun F, Pingui Z, et al. Cytokine Profiling in the Eutopic Endometrium of Adenomyosis During the Implantation Window After Ovarian Stimulation. *Reprod Sci* 2016;23:124-33.
- Guo S, Li Z, Yan L, et al. GnRH agonist improves pregnancy outcome in mice with induced adenomyosis by restoring endometrial receptivity. *Drug Des Devel Ther* 2018;12:1621-31.
- Fischer CP, Kayisili U, Taylor HS. HOXA10 expression is decreased in endometrium of women with adenomyosis. *Fertil Steril* 2011;95:1133-6.
- Du H, Taylor HS. The Role of Hox Genes in Female

- Reproductive Tract Development, Adult Function, and Fertility. *Cold Spring Harb Perspect Med* 2015;6:a023002.
19. Yong W, Ma H, Na M, et al. Roles of melatonin in the field of reproductive medicine. *Biomed Pharmacother* 2021;144:112001.
 20. Huang CC, Chiou CH, Liu SC, et al. Melatonin attenuates TNF- α and IL-1 β expression in synovial fibroblasts and diminishes cartilage degradation: Implications for the treatment of rheumatoid arthritis. *J Pineal Res* 2019;66:e12560.
 21. Reiter RJ, Tan DX, Korkmaz A, et al. Melatonin and stable circadian rhythms optimize maternal, placental and fetal physiology. *Hum Reprod Update* 2014;20:293-307.
 22. Chuffa LGA, Lupi LA, Cuciolo MS, et al. Melatonin Promotes Uterine and Placental Health: Potential Molecular Mechanisms. *Int J Mol Sci* 2019;21:300.
 23. He C, Wang J, Li Y, et al. Melatonin-related genes expressed in the mouse uterus during early gestation promote embryo implantation. *J Pineal Res* 2015;58:300-9.
 24. Institute of Laboratory Animal Resources; Commission on Life Sciences; National Research Council. *Guide for the Care and Use of Laboratory Animals*. Washington, DC: National Academy Press, 1996. Available online: https://ncbi.nlm.nih.gov/books/NBK232589/pdf/Bookshelf_NBK232589.pdf
 25. Dair EL, Simoes RS, Simões MJ, et al. Effects of melatonin on the endometrial morphology and embryo implantation in rats. *Fertil Steril* 2008;89:1299-305.
 26. Rossi AG, Soares JM Jr, Motta EL, et al. Metoclopramide-induced hyperprolactinemia affects mouse endometrial morphology. *Gynecol Obstet Invest* 2002;54:185-90.
 27. Yanar K, Simsek B, Çakatay U. Integration of Melatonin Related Redox Homeostasis, Aging, and Circadian Rhythm. *Rejuvenation Res* 2019;22:409-19.
 28. Chitimus DM, Popescu MR, Voiculescu SE, et al. Melatonin's Impact on Antioxidative and Anti-Inflammatory Reprogramming in Homeostasis and Disease. *Biomolecules* 2020;10:1211.
 29. Tang L, Zhang C, Yang Q, et al. Melatonin maintains inner blood-retinal barrier via inhibition of p38/TXNIP/NF- κ B pathway in diabetic retinopathy. *J Cell Physiol* 2021;236:5848-64.
 30. Kelleher AM, DeMayo FJ, Spencer TE. Uterine Glands: Developmental Biology and Functional Roles in Pregnancy. *Endocr Rev* 2019;40:1424-45.
 31. Richter KS, Bugge KR, Bromer JG, et al. Relationship between endometrial thickness and embryo implantation, based on 1,294 cycles of in vitro fertilization with transfer of two blastocyst-stage embryos. *Fertil Steril* 2007;87:53-9.
 32. Zhang S, Lin H, Kong S, et al. Physiological and molecular determinants of embryo implantation. *Mol Aspects Med* 2013;34:939-80.
 33. Kayo D, Zempo B, Tomihara S, et al. Gene knockout analysis reveals essentiality of estrogen receptor β 1 (Esr2a) for female reproduction in medaka. *Sci Rep* 2019;9:8868.
 34. Fang X, Wu L, Yang L, et al. Nuclear progesterin receptor (Pgr) knockouts resulted in subfertility in male tilapia (*Oreochromis niloticus*). *J Steroid Biochem Mol Biol* 2018;182:62-71.
 35. Zhang H, Li C, Wen D, et al. Melatonin improves the quality of maternally aged oocytes by maintaining intercellular communication and antioxidant metabolite supply. *Redox Biol* 2022;49:102215.
 36. Lan M, Zhang Y, Wan X, et al. Melatonin ameliorates ochratoxin A-induced oxidative stress and apoptosis in porcine oocytes. *Environ Pollut* 2020;256:113374.
 37. Wu H, Jiang K, Guo S, et al. IFN- τ Mediated Control of Bovine Major Histocompatibility Complex Class I Expression and Function via the Regulation of bta-miR-148b/152 in Bovine Endometrial Epithelial Cells. *Front Immunol* 2018;9:167.

Cite this article as: Guan X, Liu D, Zhou H, Dai C, Wang T, Fang Y, Jia Y, Li K. Melatonin improves pregnancy outcomes in adenomyosis mice by restoring endometrial receptivity via NF- κ B/apoptosis signaling. *Ann Transl Med* 2022;10(24):1317. doi: 10.21037/atm-22-5493